Finite Element Simulation of Jet Combustor Using Local Extinction Approach with in Eddy Dissipation Concept

E. Ghasemi[1,*], Soheil Soleimani[1] and M.A. Almas[1,2]

[1]*Department of Mechanical and Materials Engineering, Florida International University, Miami, FL 33199, USA*

[2]*Department of Marine engineering, King Abdulaziz University, 21589, Saudi Arabia*

Abstract: Non-premixed turbulent reacting flow in a methane-fuelled coaxial jet combustor has been studied numerically employing Reynolds Averaged Navier-Stokes (RANS) models. A Finite Element Method (FEM) based solver and Eddy Dissipation Concept (EDC) is used to simulate the methane air reaction inside the combustor. Simulations were carried out using the $k-\omega$ (k-omega) turbulence model to handle the fluid flow simulation along with heat transfer and chemical reaction. The results were compared to available LES numerical results and experimental data for predicting velocity, and temperature fields. Velocity, temperature and concentration of the different species are also plotted at different cross sections of the methane burner.

Keywords: Turbulent reacting flow, eddy dissipation concept, steady rans models, openfoam, combustor.

1. INTRODUCTION

Combustion is an interdisciplinary topic which combines the most sophisticated phenomena of fluid dynamics and chemical reactions. Combustion involves many complex phenomena, such as turbulence, recirculation, mixing, fuel chemistry, turbulence chemistry interaction and heat and mass transfer. The chemical reaction takes place in a turbulent environment where the highly unsteady fluid motions of a wide range of length and time scales are present. Turbulent combustion [1-6] interaction is one of the most complicated products of this combination. Study of turbulence effect on chemical reaction is challenging in many aspects. Comprehending of the complex effects of a macro level phenomenon (turbulence) on a molecular lever phenomenon (chemical reaction) is the main challenge [7-9]. Of particular interest is non-premixed combustion in a coaxial jet combustor configuration. It is simple yet manifests many complex flow features which are similar to those in a real gas turbine combustor. Due to increasing environmental concerns and stringent emission regulations, modern combustion engineers designing a gas turbine combustor have to face the challenge of the optimization of environmental emissions, combustion efficiency and stability. Accurate predictions of important physical and chemical properties of the combustion process are necessary in order to achieve improved combustor design with high efficiency and low emissions. As the rate of the reaction in combustion depends on the mixing rate, numerical models employed must be able to capture the mixing and unsteady flow behaviors accurately to provide an insight into the combustion process, which is of practical and technical importance. Computational Fluid Dynamics (CFD) plays an important role in designing and optimizing flow processes, especially in cases which experimental studies are not able to provide sufficient flow information due to the expensive setup cost or limitation in the measurement technology. In CFD, the combustion process is described by governing transport equations for fluid flow and heat transfer, along with models for combustion chemistry, radiation and other important sub processes. The complexity of turbulent reacting flows has led the researchers to develop various physical models. Eddy Dissipation Concept (EDC) [10,11] is one of those models for turbulence-chemistry interaction modeling in CFD. The EDC has been successfully applied to the numerical simulation of combustion for a longer period of time [12,13], and it is implemented in most commercial CFD codes available. In this work k Omega turbulence [14-16] models has been employed in modeling of turbulent reacting flow in a methane-fuelled coaxial jet combustor. Simulations have been performed in Finite Element Method based commercial software, COMSOL Multiphysics [17], and chemical reaction kinetics and combustion process is handled using Eddy Dissipation Concept (EDC).

2. GOVERNING EQUATIONS AND TURBULENCE MODELING

The compressible formulation of Reynolds Average Navier-Stokes (RANS) equations is used in this work. The governing equations at steady state are:

*Address correspondence to this author at the Department of Mechanical and Materials Engineering, Florida International University, Miami, FL 33199, USA; Tel: +1 786-202-3565; Fax: (305) 348-1932; E-mail: eghas001@fiu.edu

E-ISSN: 2409-5826/14

Continuity Equation:

$$\partial\langle\rho u_i\rangle/\partial x_i = 0 \tag{1}$$

Momentum equation:

$$\partial\langle\rho u_i\rangle\langle u_j\rangle/\partial x_i = -\partial\langle p_{eff}\rangle/\partial x_i + \frac{\partial}{\partial x_j}$$
$$\left[\mu_{eff}\left(\partial\langle u_i\rangle/\partial x_j + \partial\langle u_j\rangle/\partial x_i\right) - (2/3)\delta_{ij}\,\partial\langle u_l\rangle/\partial x_l\right] - \rho g_i \tag{2}$$

Energy equation:

$$\partial\langle\rho u_i\rangle\left(\langle E + p/\rho\rangle\right)/\partial x_j = \frac{\partial}{\partial x_j}\left[\lambda_{eff}\left(\partial\langle T\rangle/\partial x_j + \partial\langle h_i \vec{J}_j\rangle/\partial x_i\right) + \right.$$
$$\left. + \langle u_j\rangle\mu_{eff}\left(\partial\langle u_i\rangle/\partial x_j + \partial\langle u_j\rangle/\partial x_i\right) - (2/3)\delta_{ij}\,\partial\langle u_l\rangle/\partial x_l\right] + S_{chem} + S_{rad} \tag{3}$$

Species transport equations:

$$\partial\langle\rho u_i\rangle\langle Y_i\rangle/\partial x_j = \frac{\partial}{\partial x_j}\left[\left(\rho D_{i,m} + \mu_t/Sc_t\right)\right.$$
$$\left.\left(\partial\langle Y_i\rangle/\partial x_j + \partial\langle Y_i\rangle/\partial x_j\right)\right] + R_i + S_i \qquad i = 1,\ldots,\mathrm{N}-1 \tag{4}$$

Turbulent energy transport and dissipation rate equations vary based on the applied turbulence model in each simulation.

3. THE EDC FOR TURBULENT COMBUSTION

The Eddy Dissipation Concept (EDC) model [11] assumes that chemical reactions occur where the dissipation of turbulence energy takes place, that is, in the fine structures, which have characteristic dimensions that are of the order of the Kolmogorov scales. These structures are concentrated in certain regions (fine-structure regions) that occupy a fraction of the flow but not evenly distributed in time and space. In the model expressions below, different superscripts refer to states within fine structures (*), surroundings (◦), and mean values of the computational cell ($\langle\ \rangle$). The ratio of the mass of the fine structure regions to the total mass is expressed as

$$\gamma = \left(\frac{3C_{D2}}{4C^2_{D1}}\right)^{1/4}\left(\frac{\nu^*\langle\varepsilon\rangle}{\langle k^2\rangle}\right)^{1/4} \tag{5}$$

where the model constants are $C_{D1} = 0.134$ and $C_{D1} = 0.5$ and ν^* is the kinematic viscosity of the fine-structure mixture. The ratio of the mass of the fine structures to the total mass is modeled as $\gamma^* = \gamma$. Hence, the residence time in the fine structure homogeneous reactor is given as $\tau^* = 1/\dot{m}^*$. The expressions for γ, γ^* and m^{**} follows from the cascade model, which models the energy transfer from large to smaller scales. The mass-averaged mean reaction rate according to the EDC can be given as

$$-\langle S_k\rangle = \left(\left(\bar{\rho}\gamma\dot{m}^*\chi\right)/\left(1-\gamma^*\right)\right)\left(\langle Y_k\rangle - Y_k{}^*\right), \quad k = 1,\ldots,N_{species}\sqrt{a^2+b^2} \tag{6}$$

and the relationship between the mass-averaged mean state, fine-structure state and surrounding state is expressed as

$$\langle\psi\rangle = \gamma^*\chi\psi^* + \left(1-\gamma^*\chi\right)\psi^o \tag{7}$$

Here, χ is the reacting fraction of the fine structures, which depends on three aspects: probability of coexistence of the reactants, degree of heating and a limiter to the reaction due to lack of reactants. The fine-structure mass fractions $Y_k{}^*$ must be computed. In this work the local the EDC approach is used with a global one-step reaction:

$$CH_4 + s\left(O_2 + 3.76N_2\right) \longrightarrow CO_2 + \left(2\times s\right)H_2O + 3.76\times s\,N_2 \tag{8}$$

4. GEOMETRY AND BOUNDARY CONDITIONS

Numerical simulations have been performed on a methane-air burner using a 2D asymmetry model. The grid configuration is shown in Figure **1**. The geometry and boundary conditions for the coaxial jet combustor is similar to that in the experiment of Owen *et al*. [18].

The domain extends to 3 cm upstream and the length of the combustor is 100 cm. The central inflow is methane with a velocity of 0.9287 m/s. The annular inflow is a non-swirling air with a bulk velocity of 20.63 m/s. The operating pressure of the combustor is 3.8 atm. The temperature of the fuel and air are 300 K and 750 K respectively. The two inflows are separated by a thin splitter plate with the thickness of 0.018 cm. The center radius, annular outer radius and combustor radius are 3.157 cm, 4.685 cm and 6.115 cm accordingly. For turbulence conditions, hydraulic diameter and turbulent intensity have been chosen as inlet turbulent inflow conditions. In the present study, a value of 10% has been chosen for turbulent intensity.

The hydraulic diameter values for air and fuel inlets are 0.01528 m and 0.06314 m. For k and Omega,

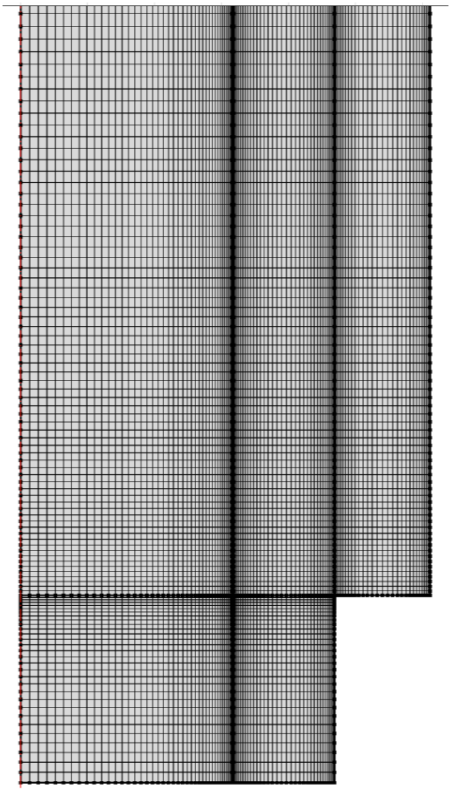

Figure 1: The geometry and grid configurations.

species and temperature the zero gradient boundary condition is applied at the outlet. The calculations were performed using steady RANS equations.

5. GRID STUDY AND VALIDATION OF NUMERICAL RESULTS

A mesh testing procedure was conducted to guarantee the grid-independency of the obtained results. Various meshes were examined for the present case as shown in Figures **2a** and **b**. As seen from the figure the total grid cell of 17820 ensures a grid-independent solution.

Figure **3** shows the comparison between the present work and previous LES [19-21] and experimental [18] results. As seen in this figure the

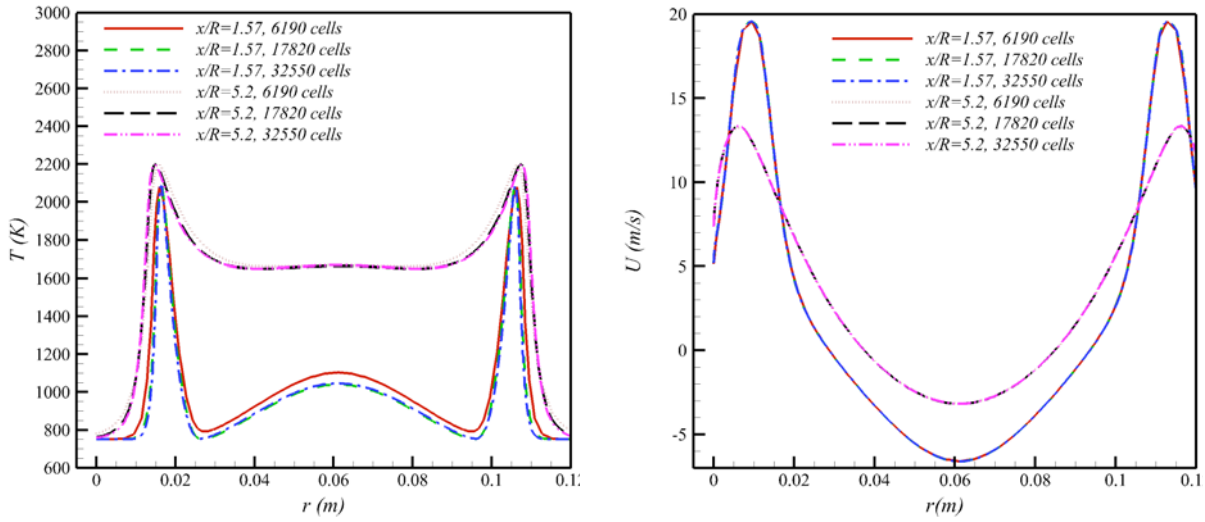

a **b**

Figure 2: Variation of (**a**) temperature and (**b**) velocity profiles for different numbers of grid cells.

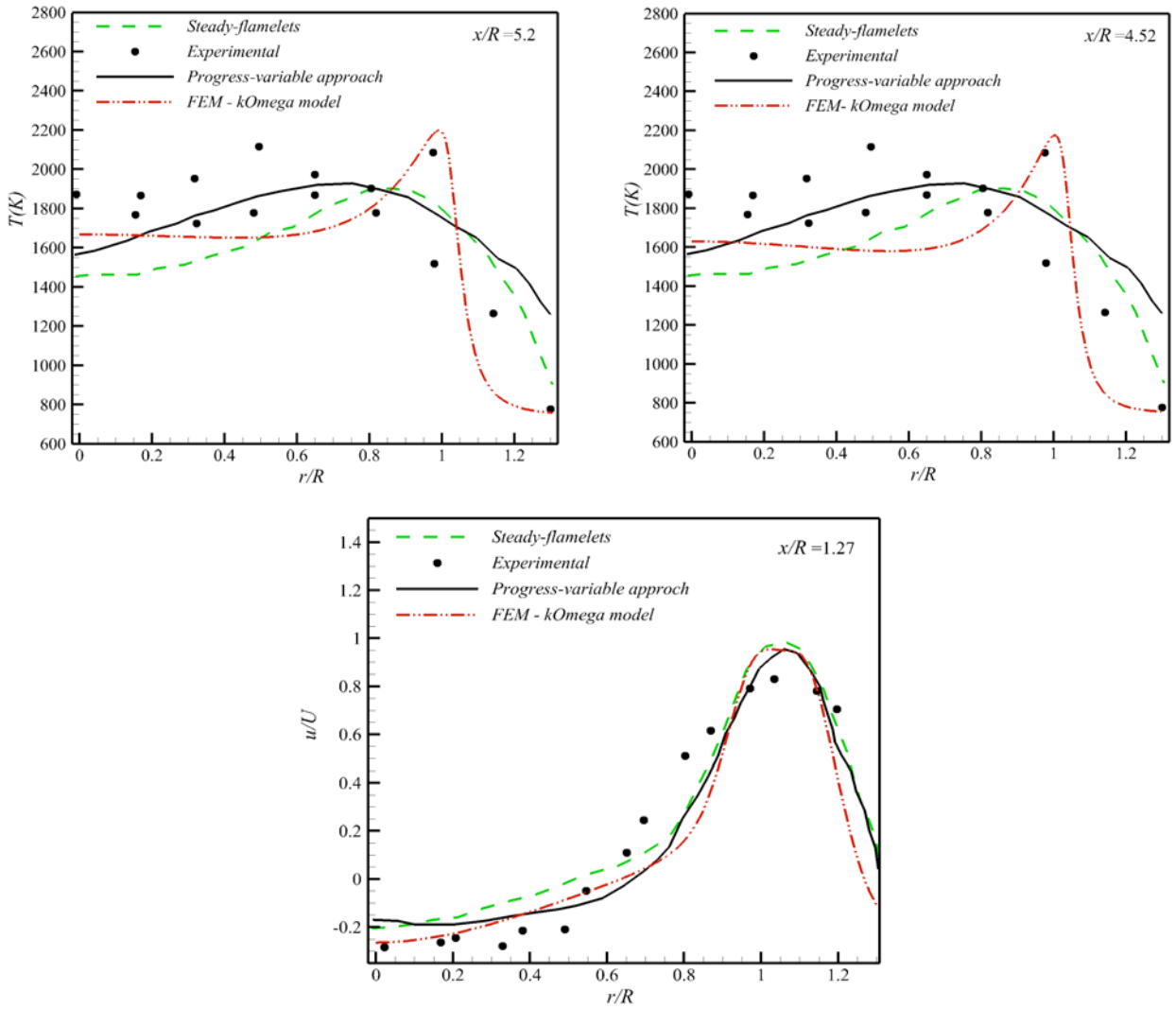

Figure 3: Comparison of the present work with previous LES [18] and experimental [17] results.

applied model in the FEM based solver could predict both temperature and velocity profile inside the combustor well.

6. RESULTS AND DISCUSSION

Steady turbulence RANS simulations results have been presented for contours of temperature, velocity in x-direction, reactant mass fractions, contours of combustion products and radial temperature and velocity profiles using COMSOL Multiphysics software.

Reactant mass fractions contours for Methane and Oxygen are shown in Figure **4**. As seen through the figures, the CH_4 concentration at the fuel inlet and Oxygen concentration at air inlet are very high. As the combustion occurs inside the combustion chamber, the concentration of both species decreases when the reactants convey further downstream of the chamber. The Oxygen concentration contour also indicates that the mass fraction of O_2 remains high adjacent to the burner's wall up to the middle of the chamber. This is because of the existence of non-reacting region near the wall where the methane does not reach these areas. The methane mass fraction contour shows that the rate of CH_4 consumption is high near the inlet where the mixing of Oxygen and Methane is high.

Figure **5** presents the temperature distribution and velocity in x-directions inside the chamber. At the inlet the value of temperature is same as reactants inlet temperatures and as the species flow downstream the chamber, combustion happens due to the mixing of air and CH_4 resulting in increase in temperature dramatically. The maximum temperature obtained at the interface of the fuel and air where the combustion has been occurred. As seen in Figure **5a** the temperature increases up to 2271 Kelvin.

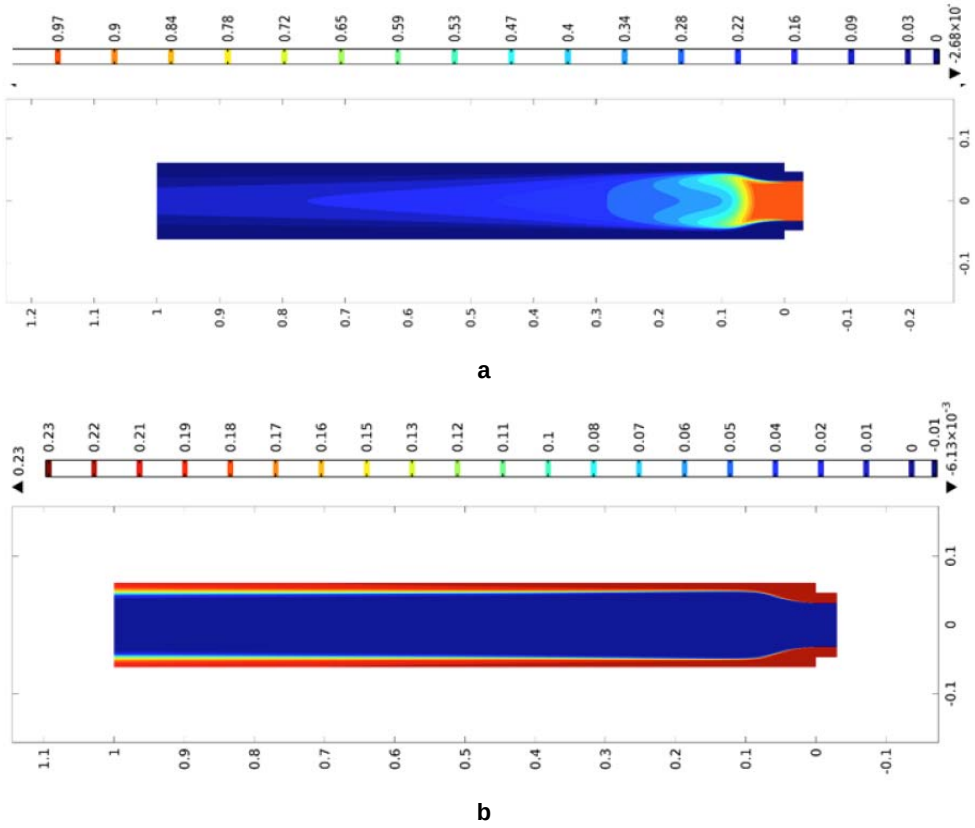

Figure 4: The contours of reactant mass fractions for (**a**) Methane, (**b**) Oxygen.

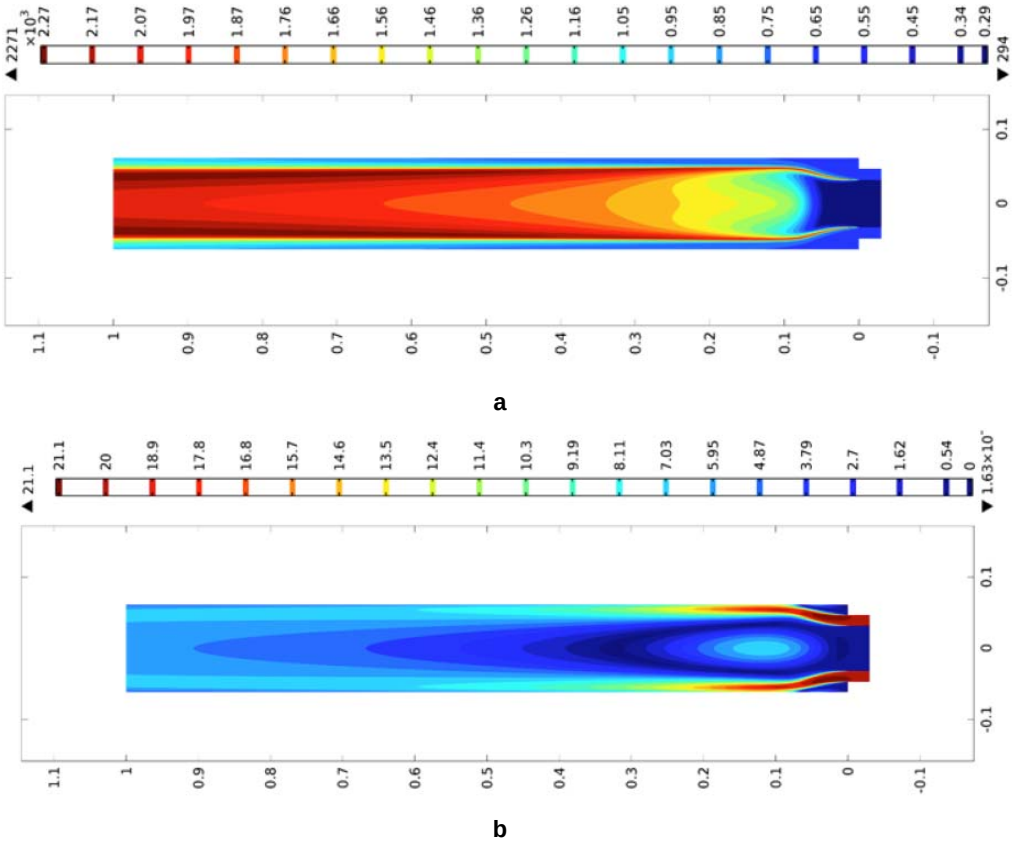

Figure 5: The contours of (**a**) temperature and (**b**) velocity in x-direction.

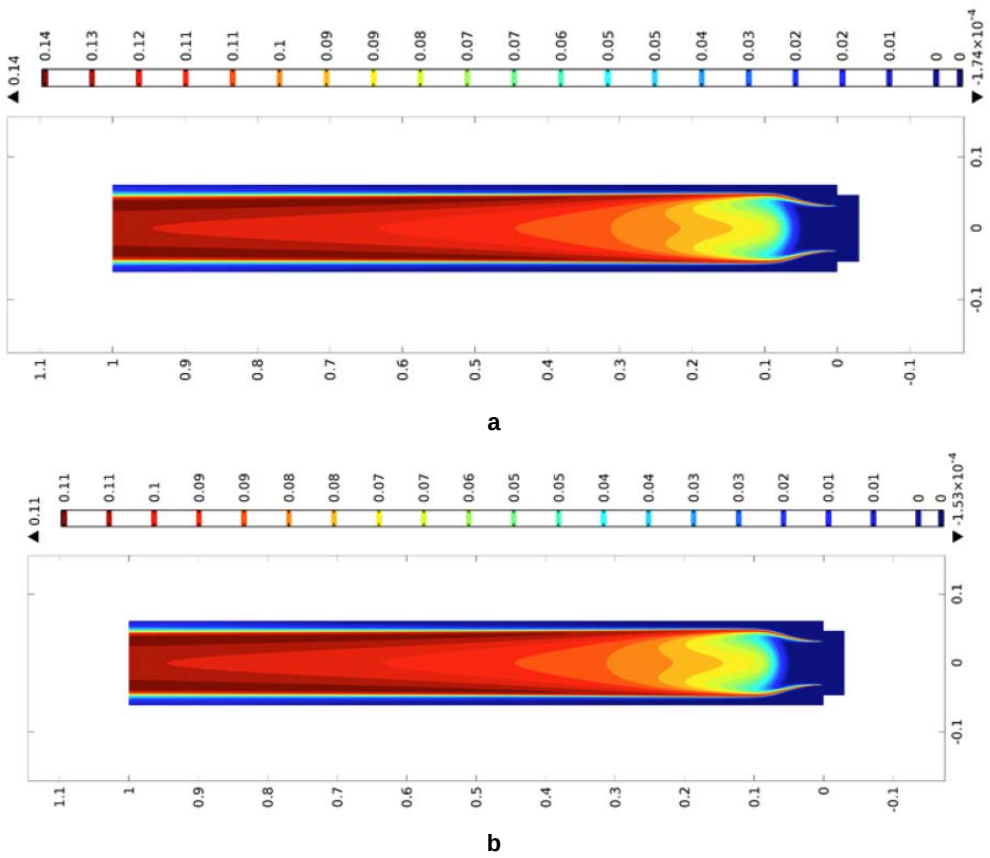

Figure 6: The contours of combustion products for (**a**) Carbon dioxide (CO_2) and (**b**) water (H_2O).

The contours of combustion products for Carbon dioxide and water have been displayed in Figure **6a** and (b). As the mixing of inlet air and CH_4 occurs, combustion happens which leads to the production of CO_2 and H_2O. Their formation trend is similar to each other as they produce after mixing of the inlet species; they also have a similar trend of temperature contour since the temperature increment has been occurred at the interface of the fuel and air in which species products (CO_2 and H_2O) form.

Figure **7** shows the concentration of different species at various cross sections of the combustor. As seen in Figures **7a** and **b** the concentration profiles of combustion products, CO_2 and H_2O, show a similar trend. Near the inlet of combustor the maximum values occurs in a small region which is the narrow reaction zone in this area where the Oxygen and Methane combustion results in the production of CO_2 and H_2O. As the flow conveys toward the outlet of the combustor, diffusion and mixing of the species make the concentration profiles of CO2 and H_2O more uniform. Moreover maximum value of the profiles is greater at the end of the combustor compared to the inlet due to more reactive processes and formation products at upstream of the outlet area. Figures **7**c shows the concentration of Oxygen at different cross section of the combustor. This figure indicates that the Oxygen concentration decreases near the outlet of combustor.

Figure **8** depicts the variation of temperature and velocity profiles at different axial locations. As seen in Figure **8a** the temperature profiles show similar trend as those in CO_2 and H_2O concentration profiles. Near the inlet of combustor the maximum temperature occurs in a small region which is the narrow reaction zone. As the flow conveys toward the outlet of the combustor the temperature profiles become more uniform. The maximum value of the temperature profiles is greater at the end of the combustor compare to the inlet area. Figure **8b** shows the velocity profiles at different cross section of the combustor. The velocity profile has its maximum value near the inlet area. In addition, as the flow approaches to the end of the combustor the maximum velocity reduces and the velocity profiles become more flat.

7. CONCLUSIONS

Turbulent reacting flow in a methane-fuelled coaxial jet combustor has been studied numerically employing steady RANS models in a finite element model based

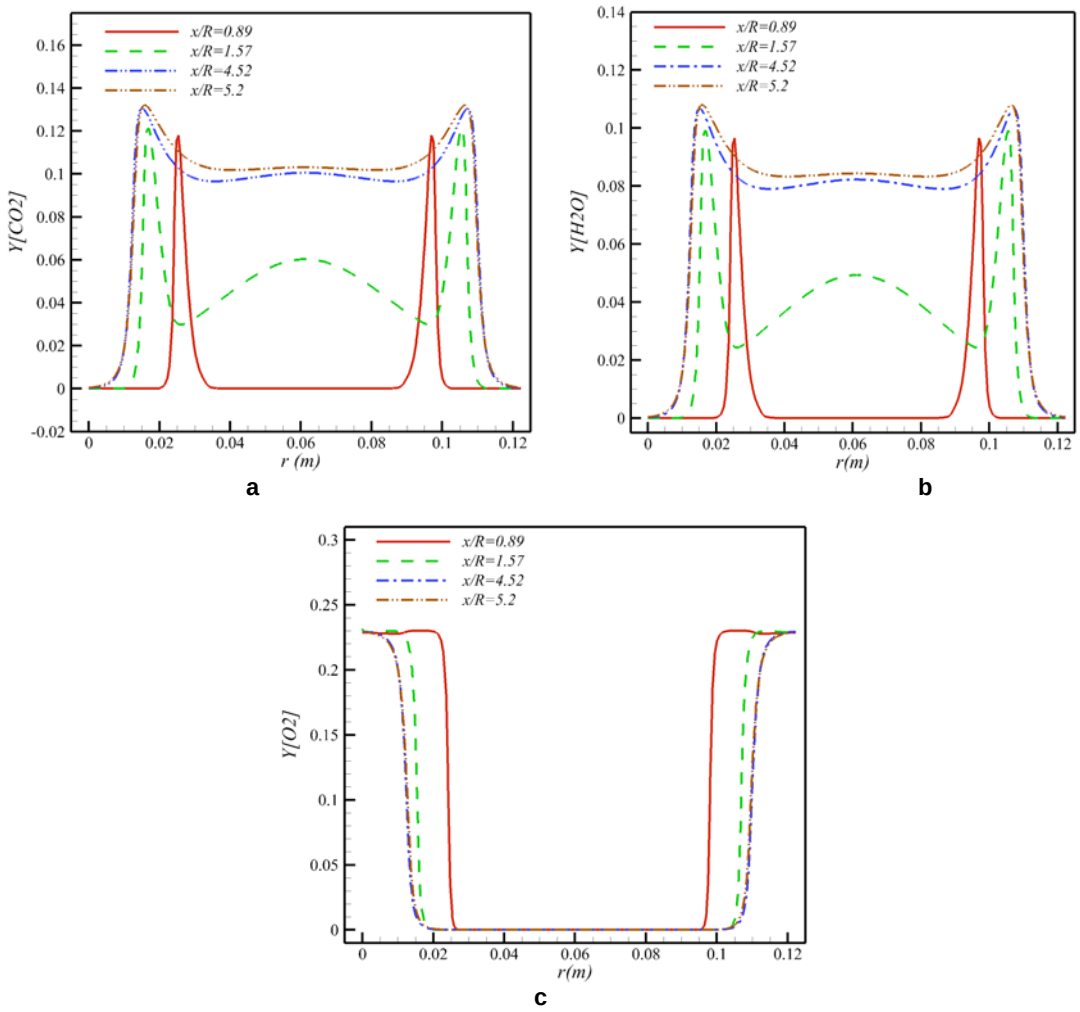

Figure 7: Concentration profiles of (a) CO_2 (b) H_2O and (c) O_2.

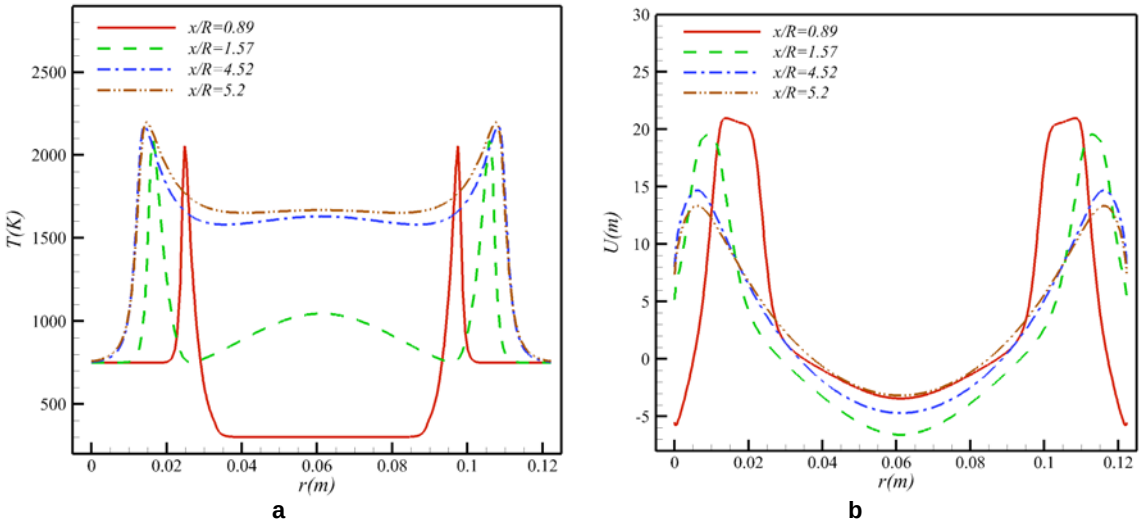

Figure 8: Temperature and velocity profile at various cross section of combustor.

solver. To simulate chemical reaction kinetics the Eddy Dissipation Concept (EDC) has been used. Results were presented for temperature, velocity in x-direction, reactant mass fractions, combustion products and radial temperature and velocity profiles. Results revealed the applicability and employed model in

prediction of heat transfer [22-39] and fluid flow field inside the combustor. As results showed, RANS models' prediction of temperature and velocity are in good agreement with experimental data and even with much lower number of grids compared to LES model.

ACKNOWLEDGMENTS

The third author would like to thank both the Saudi Arabian Cultural Mission in Washington D.C. and King Abdulaziz University in Jeddah, KSA for their support.

NOMENCLATURE

ρ	mean density (kg/m^3)
μ	molecular viscosity [kg/(m s $^{-1}$)]
μ_t	turbulent viscosity [kg/(m s $^{-1}$)]
E	total energy per unit mass (J/kg)
T	temperature (K)
S_{chem}	chemical source term in the energy equation (W/m^3)
Sc_t	turbulent Schmidt number
D	molecular diffusivity (m^2/s)
Y	mass fraction of species
C_p	specific heat at constant pressure [J/(kg K^{-1})]
v^*	kinematic viscosity of the fine-structure mixture
S_{ij}	mean strain rate tensor
τ_{ch}	chemical time (s)
χ	reacting fraction of the fine structures
$\dot{m}^*$	mass transferred between the fine structures and the surroundings

REFERENCES

[1] Agrawal GK, Chakraborty S, Som SK. Heat transfer characteristics of premixed flame impinging upwards to plane surfaces inclined with the flame jet axis. Int. J. Heat. Mass. Trans 2010; 53: 1899-1907. http://dx.doi.org/10.1016/j.ijheatmasstransfer.2009.12.068

[2] Yaga M, Endo H, Yamamoto T, Aoki H, Miura T. Modeling of eddy characteristic time in LES for calculating turbulent diffusion flame. International Journal of Heat and Mass Transfer 2002; 45: 2343-2349. http://dx.doi.org/10.1016/S0017-9310(01)00329-5

[3] Lee KW, Choi DH. Numerical study on high-temperature diluted air combustion for the turbulent jet flame in crossflow using an unsteady flamelet model. Int. J. Heat. Mass. Trans 2009; 52:5740-5750. http://dx.doi.org/10.1016/j.ijheatmasstransfer.2009.08.014

[4] Khanafer K, Aithal SM. Fluid-dynamic and NOx computation in swirl burners. International Journal of Heat and Mass Transfer 2011; 54:5030-5038. http://dx.doi.org/10.1016/j.ijheatmasstransfer.2011.07.017

[5] Yeh CL. Numerical analysis of the combustion and fluid flow in a carbon monoxide boiler. International Journal of Heat mand Mass Transfer 2013; 59:172-190. http://dx.doi.org/10.1016/j.ijheatmasstransfer.2012.12.020

[6] Saqr KM, Aly HS, Sies MM, Wahid MA. Effect of free stream turbulence on NOx and soot formation in turbulent diffusion CH4-air flames. International Communications in Heat and Mass Transfer 2010; 37:611-617. http://dx.doi.org/10.1016/j.icheatmasstransfer.2010.02.008

[7] Peters N. Turbulent Combustion, Cambridge University Press 2000. http://dx.doi.org/10.1017/CBO9780511612701

[8] Poinsot T, Veynante D. Theoretical and Numerical Combustion, Edwards Publishing 2001.

[9] Artemov V, Beale SB, de Vahl Davis G, Escudier MP, Fueyo N, Launder BE, Leonardi E, Malin MR, Minkowycz WJ, Patankar SV, Pollard A, Rodi W, Runchal A, Vanka SP. A tribute to D.B. Spalding and his contributions in science and engineering. Int. J. Heat. Mass. Trans 2009; 52:3884-3905. http://dx.doi.org/10.1016/j.ijheatmasstransfer.2009.03.038

[10] Magnussen BF. Modeling of NOx and soot formation by the Eddy Dissipation Concept. 1st topic Oriented Technical Meeting 17-19 October, Int. Flame Research Foundation, Amsterdam, Holland 1989.

[11] Magnussen BF, Hjertager BH. On mathematical modeling of turbulent combustion with special emphasis on soot formation and combustion. Proc Combust Inst 1976; 16:719-729. http://dx.doi.org/10.1016/S0082-0784(77)80366-4

[12] Gran IR, Magnussen BF. A numerical study of a bluff-body stabilized diffusion flame. Part 2. Influence of combustion modeling and finite-rate chemistry. Combust Sci Technol 1996; 119:191-217. http://dx.doi.org/10.1080/00102209608951999

[13] Myhrvold T, Ertesvåg IS, Gran IR, Cabra R, Chen JY. A numerical investigation of a lifted H2/N2 turbulent jet flame in a vitiated coflow. Combust Sci Technol 2006; 178:1001-1030. http://dx.doi.org/10.1080/00102200500270106

[14] Ghasemi E, McEligot DM, Nolan KP, Crepeau J, Tokuhiro A, Budwig RS. Entropy generation in a transitional boundary layer region under the influence of freestream turbulence using transitional RANS models and DNS. Int. Commun. Heat. Mass. Trans 2013, 41:10-16. http://dx.doi.org/10.1016/j.icheatmasstransfer.2012.11.005

[15] E.Ghasemi, D. M. McEligot, K. Nolan, J. Crepeau, A. Siahpush, R. S. Budwig, Effects of adverse and favorable pressure gradients on entropy generation in a transitional boundary layer region under the influence of freestream turbulence, Int. J. Heat. Mass. Trans 77 (2014) 475-488. http://dx.doi.org/10.1016/j.ijheatmasstransfer.2014.05.028

[16] Ghasemisahebi E. Entropy generation in transitional boundary layers. LAP LAMBERT Academic Publishing 2013.

[17] http://www.comsol.com/

[18] Owen FK, Spadaccini LJ, Bowman CT. Pollutant formation and energy release in confined turbulent diffusion flames. Proc Combust Inst 1976; 16:105-117. http://dx.doi.org/10.1016/S0082-0784(77)80317-2

[19] Pierce CD, Moin P. Progress-variable approach for large-eddy simulation of non-premixed turbulent combustion. J Fluid Mech 2004; 504:73-97. http://dx.doi.org/10.1017/S0022112004008213

[20] Taeibi-Rahni M, Ramezanizadeh M, Ganji DD, Darvan A, Ghasemi E, Soleimani S, Bararni H. Comparative study of large eddy simulation of film cooling using a dynamic global-coefficient subgrid scale eddy-viscosity model with RANS and Smagorinsky Modeling. Int. Commun. Heat. Mass. Trans 2011; 38:659-667. http://dx.doi.org/10.1016/j.icheatmasstransfer.2011.02.002

[21] Taeibi-Rahni M, Ramezanizadeh M, Ganji DD, Darvan A, Ghasemi E, Soleimani S, Bararni H. Large-eddy simulations of three dimensional turbulent jet in a cross flow using a dynamic subgrid-scale eddy viscosity model with a global model coefficient. World Appl Sci J 2010; 9:1191-1200.

[22] Ghasemi E, Soleimani S, Bararnia H, Domairry G. Influence of Uniform Suction/Injection on Heat Transfer of MHD Hiemenz Flow in Porous Media. ASCE Journal of Engineering Mechanics 2012; 138(1):82-88. http://dx.doi.org/10.1061/(ASCE)EM.1943-7889.0000301

[23] Ghasemi E , Soleimani S, Bayat M. Control Volume Based Finite Element Method Study of Nano-fluid Natural Convection Heat Transfer in an Enclosure Between a Circular and a Sinusoidal Cylinder. Int. J. Nonlinear. Scienc. Numeric. Simulation 2013; 13(7-8):521-532.

[24] Ghasemi E, Soleimani S, Bararnia H. Natural convection between a circular enclosure and an elliptic cylinder using Control Volume based Finite Element Method. Int. Commun. Heat. Mass. Trans 2012; 39:1035-1044. http://dx.doi.org/10.1016/j.icheatmasstransfer.2012.06.016

[25] Ghasemi E, Bayat M, Bayat M. Visco-Elastic MHD flow of Walters liquid b fluid and heat transfer over a non-isothermal stretching sheet. International Journal of Physical Sciences 2011; 6(21):5022-5039.

[26] Jalaal M, Ghasemi E, Ganji DD, Bararnia H, Soleimani S, Nejad GM, Esmaeilpour M, Effect of temperature-dependency of surface emissivity on heat transfer using the parameterized perturbation method. Thermal Science 2011; 15:123-125. http://dx.doi.org/10.2298/TSCI11S1123J

[27] Bararnia H, Ghasemi E, Soleimani S, Baraei A, Ganji DD. HPM-Padé method on natural convection of Darcian fluid about a vertical full cone embedded in porous media. Journal of Porous Media 2011; 14:545-553. http://dx.doi.org/10.1615/JPorMedia.v14.i6.80

[28] Bararnia H, Ghasemi E, Domairry G, Soleimani S. Behavior of micro-polar flow due to linear stretching of porous sheet with injection and suction. Advances in Engineering software 2010; 41:893-897. http://dx.doi.org/10.1016/j.advengsoft.2009.12.007

[29] Bararnia H, Ghasemi E, Soleimani S, Ghotbi AR, Ganji DD. Solution of the Falkner-Skan wedge flow by HPM-Pade'method. Advances in Engineering Software 2012; 43:44-52. http://dx.doi.org/10.1016/j.advengsoft.2011.08.005

[30] Kutanaei SS, Ghasemi E, Bayat M. Mesh-free modeling of two-dimensional heat conduction between eccentric circular cylinders. Int.l J. Phys. Scienc 2011; 6(16):4044 - 4052.

[31] Bararnia H, Jalaal M, Ghasemi E, Soleimani S, Ganji DD, Mohammadi F. Numerical simulation of joule heating phenomenon using meshless RBF-DQ method. International Journal of Thermal Sciences 2010; 49:2117-2127. http://dx.doi.org/10.1016/j.ijthermalsci.2010.06.008

[32] Seyyedi SM, Soleimani S, Ghasemi E, Ganji DD, gorji M, Bararnia H. Numerical Investigation of Laminar Mixed Convection in a Cubic Cavity by MRT-LBM: Effects of the Sliding Direction. Numerical Heat Transfer A 2013; 63:285-304. http://dx.doi.org/10.1080/10407782.2013.730456

[33] Soleimani S, Jalaal M, Bararnia H, Ghasemi E, Ganji DD, Mohammadi F. Local RBF-DQ method for two-dimensional transient heat conduction problems. Int. Commun. Heat. Mass. Trans 2010; 37:1411-1418. http://dx.doi.org/10.1016/j.icheatmasstransfer.2010.06.033

[34] Jalaal M, Soleimani S, Domairry G, Ghasemi E, Bararnia H, Mohammadi F, Barari A. Numerical simulation of voltage electric field in complex geometries for different electrode arrangements using meshless local MQ-DQ method. Journal of Electrostatics 2011; 69:168-175. http://dx.doi.org/10.1016/j.elstat.2011.03.005

[35] Soleimani S, Ganji DD, Gorji M, Bararnia H, Ghasemi E, Optimal location of a pair heat source-sink in an enclosed square cavity with natural convection through PSO algorithm. Int. Commun. Heat. Mass. Trans 2011; 38:652-658. http://dx.doi.org/10.1016/j.icheatmasstransfer.2011.03.004

[36] Moghimi SM, Domairry G, Bararni H, Ghasemi E, Soleimani S. Application of homotopy analysis method to solve MHD Jeffery-Hamel flows in non-parallel walls. Advances in Engineering Software 42 (2011) 108-113. http://dx.doi.org/10.1016/j.advengsoft.2010.12.007

[37] Moghimi SM, Domairry G, Bararni H, Soleimani S, Ghasemi E. Numerical Study of Natural Convection in an Inclined L-shaped Porous Enclosure. Adv Theor Appl Mech 2012; 5:237 - 245.

[38] Ganji DD, Bararnia H, Soleimani S, Ghasemi E. Analytical solution of the magneto-hydrodynamic flow over a nonlinear stretching sheet. Modern Phy. Letter B 2009; 23:2541-2556. http://dx.doi.org/10.1142/S0217984909020692

[39] Soleimani S, Ganji DD, Ghasemi E, Jalaal M, Bararnia H. Meshless local RBF-DG for 2-D heat conduction: A comparative study. Thermal Science 2011; 15:117-121.

Received on 07-10-2014 Accepted on 23-10-2014 Published on 09-01-2015

DOI: http://dx.doi.org/10.15377/2409-5826.2014.01.02.4